International Journal of Fluid Machinery and Systems
Vol. 9, No. 3, July-September 2016
DOI: http://dx.doi.org/10.5293/IJFMS.2016.9.3.256
ISSN (Online): 1882-9554

Original Paper

Design and performance research of a mixed-flow submersible deep well pump

Qihua Zhang, Yuanhui Xu, Li Cao, Weidong Shi and Weigang Lu

National Research Center of Pumps, Jiangsu University
301 Xuefu Road, Zhenjiang, 212013, P.R. China, qhzhang@mail.ujs.edu.cn

Abstract

To meet the demand of higher handling capacity, a mixed-flow submersible deep well pump was designed and tested. The main hydraulic components are made of plastics, which is free of erosion, light-weight, and environment-friendly. To simplify plastic molding process, and to improve productivity, an axial-radial guide vane was proposed. To clarify its effect on the performance, a radial guide vane and a space guide vane are developed as well. By comparison, the efficiency of the pump equipped with the axial-radial guide vane is higher than the radial guide vane and is lower than the space guide vane, and its high efficiency range is wide. The static pressure recovery of the axial guide vane is a bit lower than the space guide vane, but it is much larger than the radial guide vane. Taking the cost and molding complexity into consideration, the axial-radial guide vane is much economic, promoting its popularity for the moderate and high specific speed submersible deep well pumps.

Keywords: submersible deep well pump, mixed-flow, axial-radial guide vane, design.

1. Introduction

To keep livestock in regions lacking visible ground water, it is necessary to explore and utilize the underground water sources. For example, in middle-western and northern areas of China, deep wells are widely deployed to keep livestock, and irrigate farms as well. The well is very deep and is commonly exploited by using a pump driven by electric power, wind, solar, etc. In addition, in offshore oil deposit development, we foresee an increasing demand for oil deep well pumps. The increasing market promotes a new wave of research and development of the submersible deep well pumps.

Compared to rotating components, i.e., impeller, shaft, bearing, etc., guide vane is a stationary component, and it is rarely investigated. However, it mainly contributes to the static pressure recovery and affects the stage performance [1]. Even more, guide vane plays an important role in removing pump vibration, hydraulic excitation, and noise for a full range of operation [2-6]. By the LES simulations, Li et al.[7] investigated the transient flow through the guide vane of a mixed-flow pump, and analysed pressure fluctuation and eddy evolution. Li et al.[8] developed a low-specific mixed-flow pump for large head and capacity handling, where a return channel type of guide vane was designed. By repeated revisions of impeller blade and guide vane shape, an optimization design was obtained by analysing the flow fields via CFD. Their revision process was conducted in UGNX7.5, but the related design process was not mentioned. Lugovaya et al.[9] presented two types of guide vanes which differs a little at the transition shape of the intermediate stage cross-section, and they compared the performance of the pump equipped with these guide vanes separately. But they did not come into an exact conclusion that one outperformed another, nor did they describe how to design these guide vanes. Weiten et al.[10] investigated a small stage of radial multistage pump equipped with a single guide vane without radial diffuser, and compared with a common guide vane with radial diffuser, the test showed that the small stage efficiency was relatively lower. However, the small stage head was larger and the axial thrust was relatively smaller. Kim et al.[11] performed an optimization of a mixed-flow pump by adjusting the meridional shapes of flow path. Kim et al.[12] optimized a mixed-flow pump by parameterizing the straight vane length ratio and diffusion area ratio. Recently, Zhang et al.[13] developed a compact submersible deep well pump, where a circumferential twisted return guide vane was proposed, and its designing process was presented as well. The pump was made of casting steel and is relatively heavy and expensive.

In recent years, the environment-friend techniques are increasingly addressed. Wang et al.[14] designed an axial tidal turbine by composites. This technique is free of sea water erosion, promoting a new trend for environment protection. Recently, a series of plastic deep well pumps have been developed and occupied a major part of market share. Zhang et al.[15] presented the main technologies established during the development of these plastic pumps. Meanwhile, the demand for mixed-flow pump handling larger flow rate is

Received November 18 2014; revised August 8 2015; accepted for publication September 10 2015: Review conducted by Hyung Hee Cho. (Paper number O14032K)
Corresponding author: Qihua Zhang, Ph.D, qhzhang@mail.ujs.edu.cn

increasing. To meet the demand, a mixed-flow pump of moderate to large specific speed was developed in this paper. By improving the performance of the pump, a radial-axial return guide vane was designed where the vane is shaped with two dividing parts. Meanwhile, a radial guide vane and a space guide vane were designed to compare and clarify their effects on pump performance.

2. Guide Vane Design

2.1 Space Guide Vane

To date, there are two major types of guide vanes for submersible multistage pumps. One type is based on the cylindrical shape, the other is based on the space guide vane. The former type is always cylindrical and is mostly constructed by composite molding process. But the latter type is always fully twisted and mainly casted by iron or steel, as shown in Fig.1.

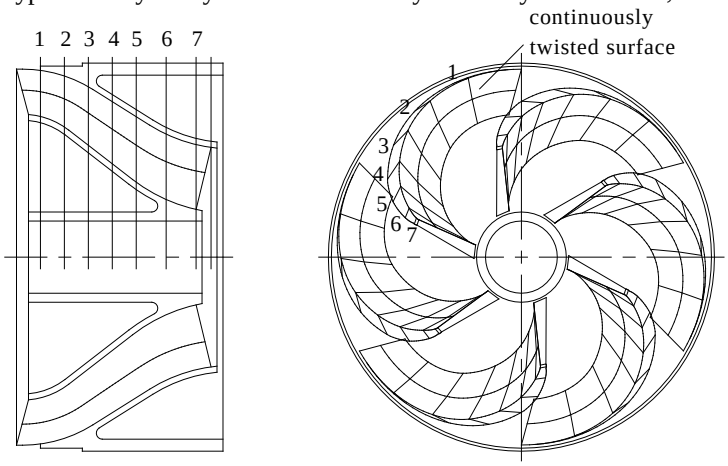

Fig. 1 Schematic of a space guide vane

For the purpose of light-weight, cheap, and easy to manufacture, these composite components are increasingly adopted in mass production of submersible multistage pumps, substituting old iron-, or steel- type pumps. On the other hand, the surface roughness of plastic component is smoother, and leading to better hydraulic performance. With outcome of 3D printing technology, the composite process will promote a prompt development of hydraulic components.

2.2 Axial-Radial Guide Vane

As shown in Fig.1, the surface of space guide vane is fully twisted. The technique involved in the molding process is rather complex, and its productivity is low. To overcome the molding difficulty, an axial-radial guide vane is proposed and its shape is depicted in Fig.2.

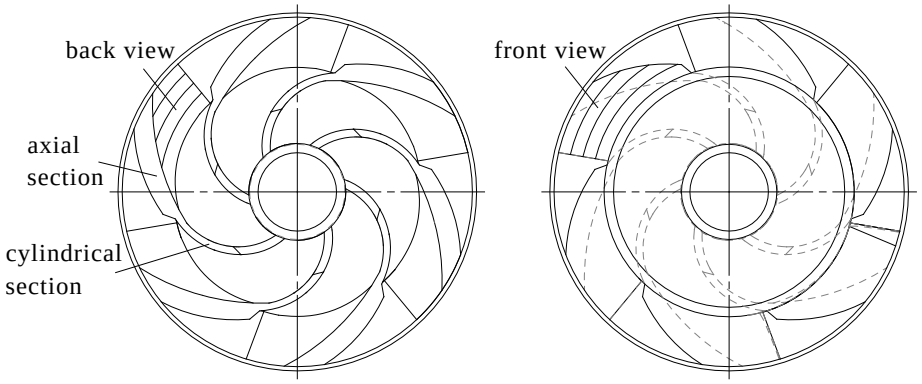

Fig. 2 Schematic of an axial-radial guide vane

As shown in Fig.3, the axial-radial guide vane is divided into two parts, where a dividing line separates the axial part and the radial part. It is noticed that this dividing line functions as a molding separation line, from which the axial and radial parts depart and the molding process becomes quite simple.

For the axial part, the blade is designed by a series of profiles obtained by the sequential cross sections, i.e., 1 to 7, as shown in Fig.3(a). Those profiles can be plotted in two separated drawings, as shown in Fig.3(b) and (c), which represents the front and back surface of the axial part.

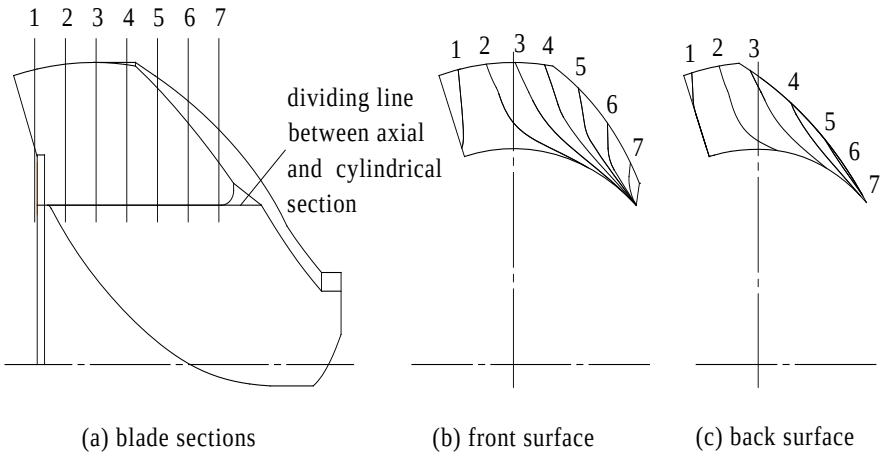

Fig. 3 Design process for the axial-radial guide vane

Subsequently, the front and back surfaces and the cylindrical parts can be plotted in a single drawing, thus a single blade layout is plotted, as shown in Fig.4.

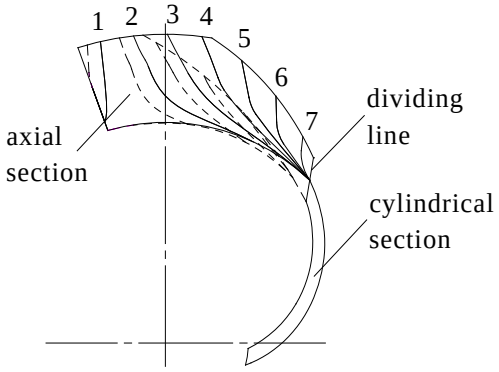

Fig. 4 Blade layout of the axial-radial guide vane

Fig. 5 Plastic sample of the axial-radial guide vane

As the original demand, a pump working at flow rate $Q = 20m^3 / h$, stage head $H = 7.5m$, and rotating speed $n = 2850r / \min$ was developed by plastic molding. And a plastic sample of the axial-radial guide vane is shown in Fig.5.

3. Numerical Investigation of Pump Performance

3.1 Model Configurations

Further, a radial guide vane and a space guide vane were developed as shown in Fig.6. And the main dimensions (hub diameter, shroud diameter, blade number, inlet blade angle, outlet blade angle, etc.) of the radial guide vane and space guide vane are identical to the axial-radial guide vane.

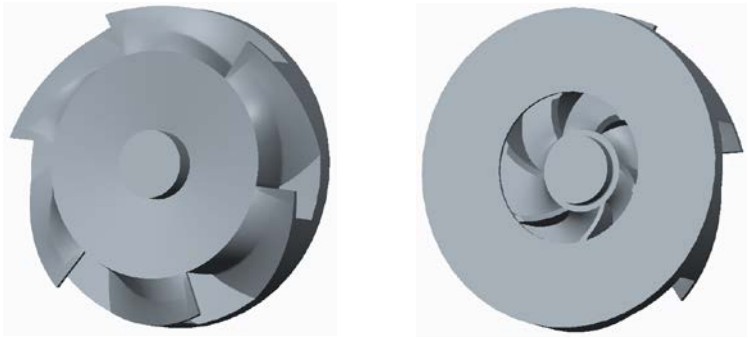

(a) axial-radial guide vane

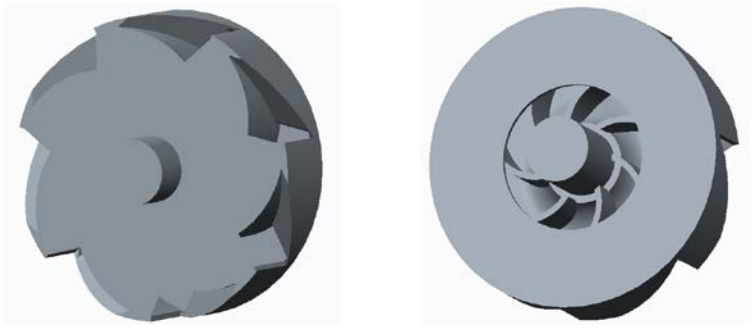

(b) radial guide vane

(c) space guide vane

Fig. 6 3D models of three types of guide vanes

The three types of guide vanes are assembled with an identical impeller, respectively. And the configurations are similar, as depicted in Fig.7. A dual-stage model is set up which includes the suction pipe, the first stage, the second stage, and the discharge pipe.

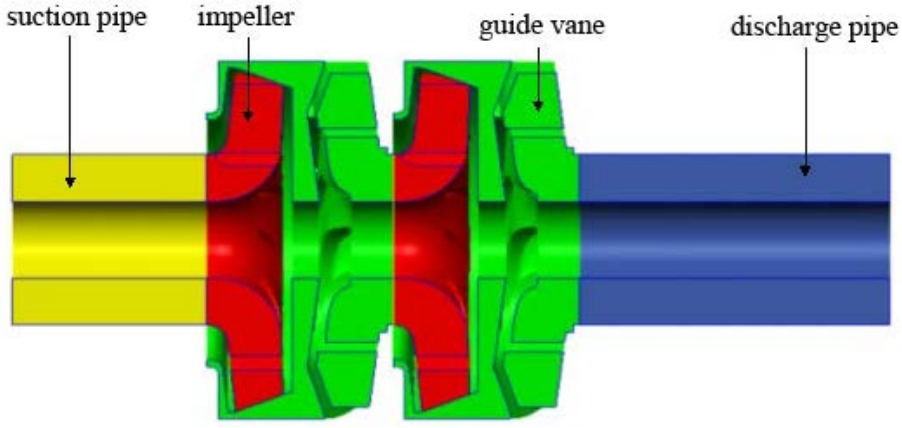

Fig. 7 Configuration of a two-stage calculation model

3.2 Computational Grids

For the purpose of precision, convergence property, and stability of numerical scheme, the structured grids are set up by ICEMCFD. And the grids of three types of configurations are depicted in Fig.8.

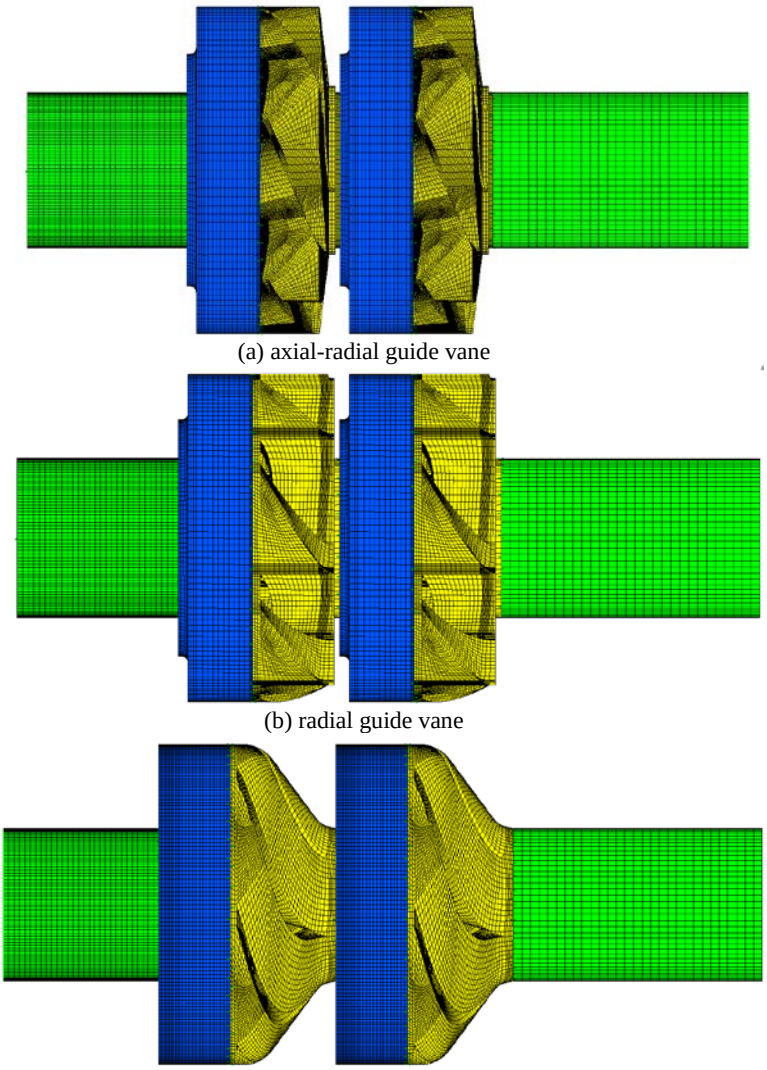

(a) axial-radial guide vane

(b) radial guide vane

(c) space guide vane

Fig. 8 Numerical grids of three configurations

For better numerical precision, the grids near walls were carefully adjusted to keep yplus value distributed within the range [30, 200]. Then the grid irrelevance was tested and optimized. Then the final grids are shown in Fig.8. Based on these grids, the subsequent simulations of the three types of configurations were conducted hereafter.

3.3 Governing Equations

For the steady incompressible flows within pumps, the mass and momentum equations are

$$\nabla \cdot \boldsymbol{u} = 0 \tag{1}$$

$$\nabla\left(\rho u \boldsymbol{u}\right) = -\nabla p + \mu \nabla^2 \boldsymbol{u} - \rho\left[2\boldsymbol{\omega} \times \boldsymbol{u} + \boldsymbol{\omega} \times \left(\boldsymbol{\omega} \times \boldsymbol{r}\right)\right] \tag{2}$$

where $\boldsymbol{u}$ is velocity vector, p is pressure, $-2\boldsymbol{\omega} \times \boldsymbol{u}$ is Coriolis force, $-\boldsymbol{\omega} \times \left(\boldsymbol{\omega} \times \boldsymbol{r}\right)$ is centrifugal force, $\boldsymbol{\omega}$ is angular velocity vector, and $\boldsymbol{r}$ is radius vector. ∇ is Cartesian differential operator.

For the demand of computational cost and efficiency, the standard $k-\varepsilon$ model was mostly adopted in simulation of pump fl ows. Based on this model, a uniform CFD configuration was setup in the ANSYS CFX, where a dual-stage calculation model was setup and the frozen rotor method was adopted to coupling the rotor-stator flow interfaces.

3.4 CFD Setup and Boundary Conditions

The simulations were performed on the platform of ANSYS CFX. For the three types of calculation models, a uniform CFD configuration was setup, where the inlet boundary condition is set by averaged suction velocity, i.e., $U_{\text{suc}} = 4Q / \pi\left(D_1^2 - D_h^2\right)$, and D_1 is impeller suction diameter, and D_h is the impeller hub diameter. And the flow at the outlet of the pump is assumed to be fully developed. And the standard $k-\varepsilon$ turbulent model was enabled for all these three configurations. And the other settings are kept default as CFX recommended.

4. Performance Simulation and Analysis

A series of simulations were conducted. Based on the numerical simulations, the stage head is calculated as follows

$$H = \frac{\left(P_{\text{tot}_{\text{dis}}} - P_{\text{tot}_{\text{suc}}}\right)}{\rho g} \tag{3}$$

Where $P_{\text{tot}_{\text{dis}}}$ is the stage total pressure of pump discharge, and $P_{\text{tot}_{\text{suc}}}$ is the stage total pressure of pump suction. Then the stage efficiency is calculated as follows

$$Eff = \frac{\rho g Q H}{M \omega} \tag{4}$$

Where M is the stage torque of the pump impeller, and ω is the rotating angular velocity of the impeller.

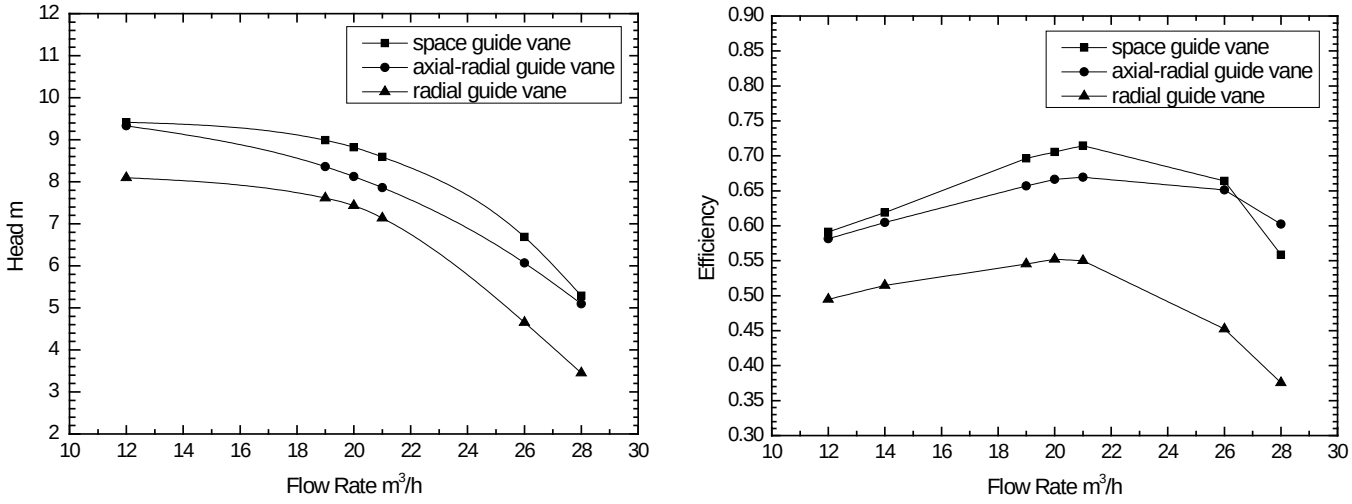

(a) Head vs. Flow rate curves

(b) Efficiency vs. Flow rate curves

Fig. 9 Pump performance curves

The simulation results are plotted in Fig.9. It is clear that the performance of the pump equipped with the axial-radial guide vane is better than the radial guide vane and is worse than the space guide vane. Especially, at large flow rate, the pump performance of axial-radial guide vane roughly equals to the space guide vane, and behaves much better than the radial guide vane.

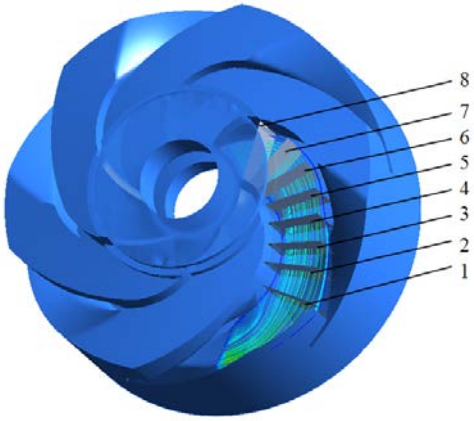

Fig. 10 Cross sections along flow channel of guide vane

Then a series of cross sections from guide channel inlet to outlet are constructed to investigate the flow field within the guide vane, as shown in Fig.10. And the area averaged static pressure and total pressure are calculated and plotted in Fig.11.

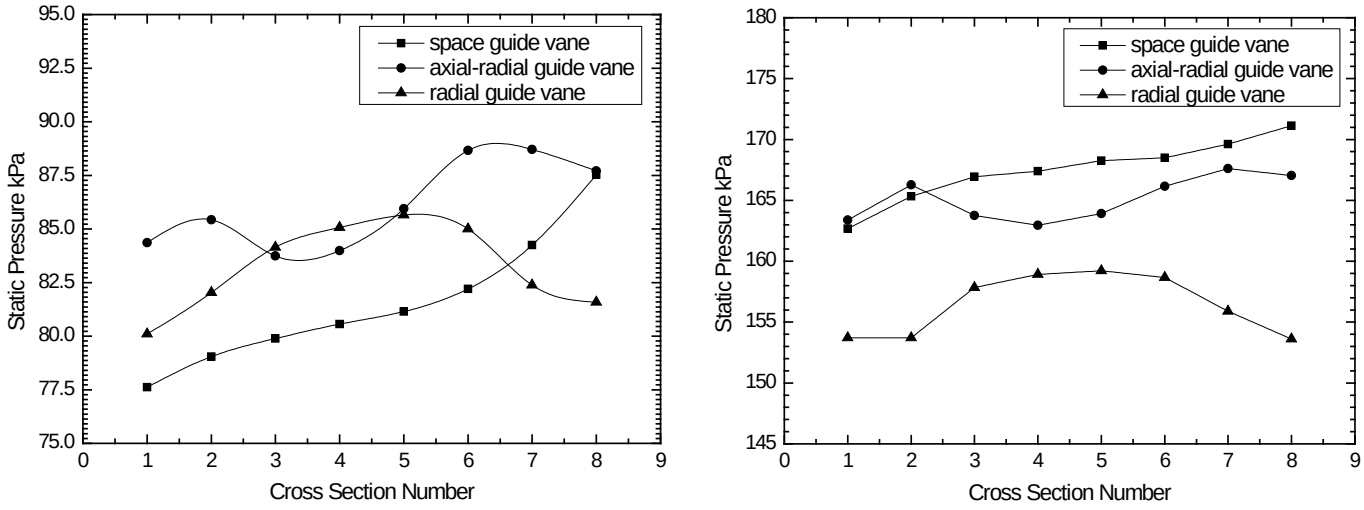

(a) first stage (b) second stage

Fig. 11 Static pressure of first stage and second stage

From Fig.11, the static pressure of the space guide vane shows a smooth increase from guide vane inlet to outlet. But the static pressure of the radial guide vane increases rapidly across the first five sections, and it decreases gradually and become very small at the outlet. The static pressure of the axial-radial guide vane is non-monotonous within the first stage, but it becomes relatively smooth in the second stage. It is noticed that, at the outlet, the space guide vane and the axial-radial guide vane nearly obtain an equal static pressure recovery level, but the pressure level of the radial guide vane is generally much lower.

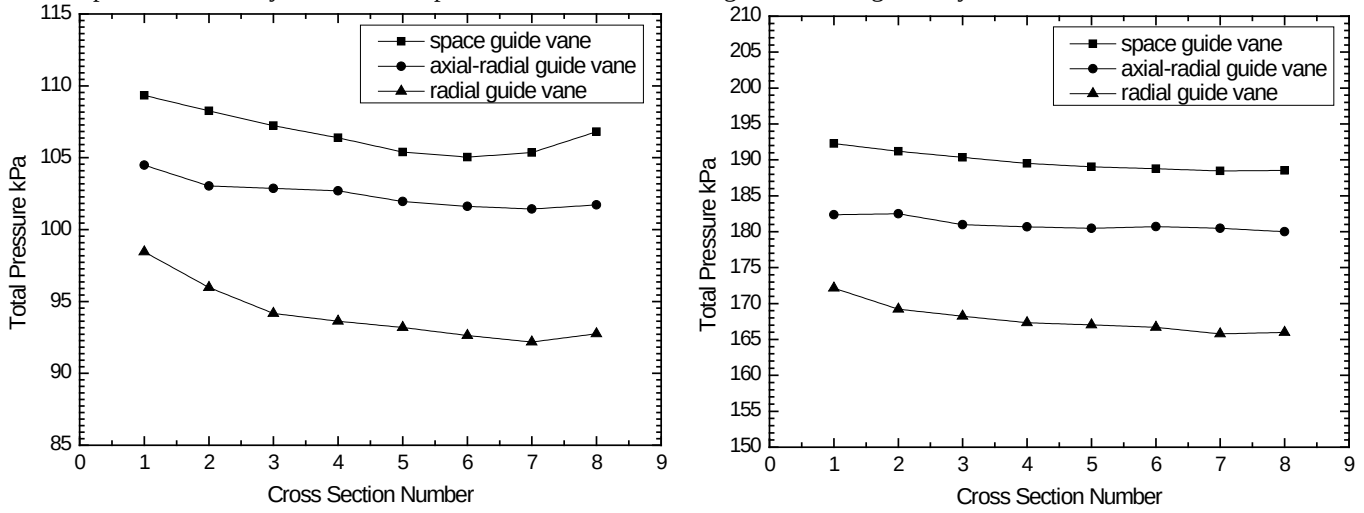

(a) first stage (b) second stage

Fig. 12 Total pressure of first stage and second stage

As shown in Fig.12, the total pressure of space guide vane is largest, and the axial-radial guide vane is a bit lower than the space guide vane, but the radial guide vane is much lower. Relatively, the total pressure loss is smaller for space guide vane and axial-radial guide vane, but it is much larger for the radial guide vane.

As shown in Fig.13, the turbulent energy level is lowest for the space guide vane, and it is largest for the axial guide vane. And it is noticed that, the turbulent energy of the axial-radial guide is mainly concentrated on the inlet region, and it gradually decreases toward the outlet. However, the turbulent energy of radial guide vane is much larger across the whole flow channel, leading to larger total pressure loss.

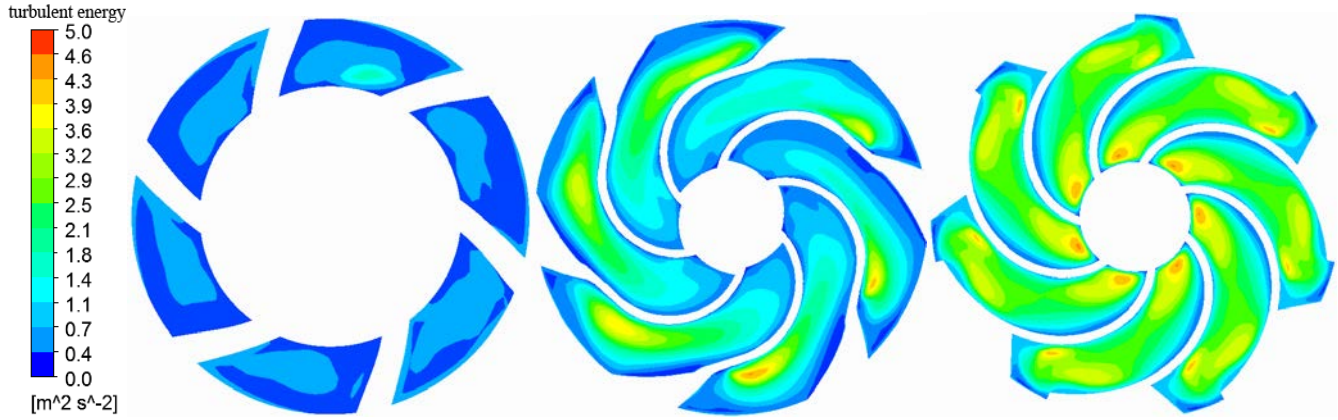

Fig. 13 Turbulent energy distributions for three guide vanes

5. Conclusion

To exploit underground water resource, the deep wells are commonly used in farms, mountain and desert areas, etc. Furthermore, oil field exploration shows a growing tendency in recent years. To meet the demand, especially for the moderate to high specific speed range, a mixed-flow submersible deep well pump is developed in this study. The main components of the pump were developed by plastics. With a relatively low rotating speed, the composite components can commonly meet the strength level up to 5 inch diameter.

To simplify molding process and improve productivity, an axial-radial guide vane was proposed. To examine its performance, a space guide vane and a radial guide vane were developed for comparison. The numerical simulations were performed to compare and analyze their differences. Firstly, the performance characteristic curves were obtained from the simulations, and it shows that the performance of the axial-radial guide vane is roughly equal to the space guide vane, and it is much better than the radial guide vane. Secondly, a series of cross sections along the flow channel are arranged to monitor the pressure recovery of the three guide vanes. It shows that the outlet static pressure of space guide vane and axial-radial guide vane is much closer, but the radial guide vane is much lower. And the total pressure loss and turbulent energy of the space guide vane is lowest, and the difference between the space guide vane and the axial-radial guide vane is small, but the gap between the space guide vane and the radial guide vane is largest.

Totally, the mixed-flow submersible deep well pump developed in this study is economic. Especially, with the axial-radial guide vane, the plastic molding process is simplified and the productivity is greatly improved, reducing its mass production cost. Meanwhile, it is a environment-friendly technique for non-erosion. Furthermore, minor revisions can be further made to improve inlet blade shape of the axial-radial guide vane, thus the total pressure loss can be further reduced.

Acknowledgments

The authors are grateful for the financial support by the National Natural Science Foundation of China (No. 51309118), the National Natural Science Foundation of Jiangsu Province (No. BK20130527), and the six talent peaks project in Jiangsu Province (NO. 2015-ZBZZ-016).

Nomenclature

D_1	Impeller suction diameter[mm]	M	Stage torque of impeller [Nm]
D_h	Impeller hub diameter[mm]	n	Rotating speed of impeller [r/min]
g	Total pressure [Pa]	$\boldsymbol{u}$	Velocity vector
H	Gravitational acceleration	ω	Rotating angular velocity of impeller (rad/s)
p	Pressure [Pa]	U_{suc}	Velocity of impeller suction eye
P_{tot}	Stage head [m]	ρ	Fluid Density
Q	Flow rate of pump [m^3/h]		

References

[1] Tan, L., Cao, S. L., and Gui, S. B., 2010, “Hydraulic Design and Pre-whirl Regulation Law of Inlet Guide Vane for Centrifugal Pump,” Science China Technological Sciences, Vol. 53, No. 8, pp. 2142-2151.

[2] Clemen, C., 2011, “Aero-mechanical Optimization of a Structural Fan Outlet Guide Vane,” Structural and Multidisciplinary Optimization, Vol. 44, No. 1, pp. 125-136.

[3] Kawashima, D., Kanemoto, T., and Sakoda, K., 2008, “Matching Diffuser Vane with Return Vane Installed in Multistage Centrifugal Pump,” The International Journal of Fluid Machinery and Systems, Vol. 1, No. 1, pp. 86-91.

[4] Chernoray, V., Ore, S., and Larsson, J., 2010, “Effect of Geometry Deviations on the Aerodynamic Performance of An Outlet Guide Vane Cascade,” Proceedings of ASME Turbo Expo 2010: Power for Land, Sea, and Air, pp. 381-390.

[5] Pavesi, G., Ardizzon, G., and Cavazzini, G., 2004, “Numerical and Experimental Investigations on A Centrifugal Pump with and Without A Vaned Diffuser,” IMECE2004-59544.

[6] Devals, C., Vu, T.C., Guibault, F., 2015, “CFD analysis for Aligned and Misaligned Guide Vane Torque Prediction and Validation with Experimental Data,” The International Journal of Fluid Machinery and Systems, Vol. 3, No. 3, pp. 132-141.
[7] Li, Y. B., Li, R.N., and Wang, X.D., 2013, “The Numerical Simulation of Unsteady Flow in a Mixed flow Pump Guide Vane,” The International Journal of Fluid Machinery and Systems, Vol. 6, No. 4, pp. 200-205.
[8] Li, H. F., Huo, Y. W., Pan, Z. B., Zhou, W. C., and He, M. H., 2012, “Development and Numerical Analysis of Low Specific Speed Mixed-flow Pump,” IOP Conf. Series: Earth and Environmental Science, Vol. 15, 032017.
[9] Lugovaya, S., Olshtynsky, P., Rudenko, A., and Tverdokhleb, I., 2012, “Revisited Designing of Intermediate Stage Guide Vane of Centrifugal Pump,” Procedia Engineering, Vol. 39, pp. 223-230.
[10] Weiten, A., and Hellmann, D.-H., 2006, “Investigation of a Centrifugal Pump Stage with Radial Impeller and a pump Stage with Small Stage Diameter,” Proceedings of IMECE2006, IMECE2006-14258.
[11] Kim, S., Choi, Y.S., Lee, K.Y., Kim, J.H., 2011, “Design Optimization of Mixed-flow Pump in a Fixed Meridional Shape,” The International Journal of Fluid Machinery and Systems, Vol. 4, No. 1, pp. 14-24.
[12] Kim, J.H., Kim, K.Y., 2011, “Optimization of Vane Diffuser in a Mixed-Flow Pump for High Efficiency Design,” The International Journal of Fluid Machinery and Systems, Vol. 4, No. 1, pp. 172-178.
[13] Zhang, Q. H., Shi, W. D., Xu, Y., Gao, X. F., Wan, C., Lu, W. G., and Ma, D. Q., 2013, “A New Proposed Return Guide Vane for Compact Multistage Centrifugal Pumps,” International Journal of Rotating Machinery, Vol. 2013, 683713.
[14] Wang, J. F., Patil, M., Olortegui-Yume, and J., Müller, N., 2010, “Mechanical Design of Wound Composite Impeller Using FEM,” Proceedings of IMECE2010, IMECE2010-39762.
[15] Zhang, Q. H., Xu, Y., Xu, Y. H., Shi, W. D., Lu, W. G., Liu, W., 2013, “Study on Key Technologies of Energy-Saving and Environment-Protective Pumps,” Thermal Science, Vol. 17, No. 5, pp. 1556-1559.